https://doi.org/10.5194/acp-2022-364
Preprint. Discussion started: 30 May 2022

Atmospheric Chemistry and Physics Discussions

Water uptake and the gas-particle partitioning of nitrate aerosols

Hoang Duong Do[1,2,a], Yong Bin Lim[3], Yong Pyo Kim[3]

[1]Department of Energy and Environment Engineering, University of Science and Technology, Daejeon, 34113, South Korea
[2]Environment, Health, and Welfare Research Center, Korea Institute of Science and Technology, Seoul, 02792, South Korea.
[a]now at: Institute of Energy and Climate Research: Troposphere (IEK-8), Forschungszentrum Jülich GmbH, Jülich, Germany
[3]Department of Chemical Engineering and Material Science, Ewha Womans University, Seoul, 03760, South Korea

Correspondence to: Yong B. Lim (ylim@ewha.ac.kr)

Abstract. Nitrate uptake into particles is an important feature of thermodynamic equilibriums responsible for the high-concentration particle formation in East Asia. However, key processes including the gas-particle partitioning of HNO_3-NO_3^- and the deliquescence of particles, are not scrutinized in thermodynamic model simulations used in field studies. Using a humidified tandem differential mobility analyzer (HTDMA), we investigated water uptake and gas-particle partitioning of nitrates for inorganic and inorganic-organic aerosols as we simulated thermodynamic models (ISORROPIA-II and E-AIM). For the best-fit to HTDMA measurements, we revised thermodynamic model simulations and conducted linear regressions. Results demonstrated that ammonium nitrate aerosols maintained deliquescence in the entire range of 10-90% relative humidity (RH) and in the range of 30-70% RH the aerosol liquid water content (ALWC) and nitrates in ammonium-sulfate-nitrate aerosols simultaneously evaporated. Glyoxal exhibited hygroscopicity and a synergetic effect on ALWC formation with ammonium sulfates. In ammonium-sulfate-nitrate-glyoxal aerosols, more ALWC and nitrates formation above 50% RH is likely due to the synergetic effect among ammonium, sulfates and nitrates. Considering that 30-80% RH is haze conditions in East Asia, we propose that pronounced nitrate formation in particles beyond the description of current thermodynamic model simulations includes deliquescent nature of ammonium nitrate aerosols that undergo hysteresis with an unclear efflorescence RH point due to incomplete equilibriums, the evaporation of ALWC, nitrates and ammoniums in sulfate-rich aerosols, and the synergetic effect between organic and inorganic components on ALWC formation at high RH.

1 Introduction

Nitrate uptake into particles is a key mechanism for the formation of particulate matter (PM) in urban areas, particularly during high-concentration PM events. The summertime haze in the North China Plain (NCP) was driven by nitrate production through co-condensation of ammonia and nitric acid, suggesting ammonia reduction to be an effective strategy for PM mitigation (Li et al., 2018). This ammonia reduction strategy based on the co-condensation of ammonia and nitric acid was also suggested by Guo et al.'s global study (Guo et al., 2018). In addition to the co-condensation with ammonia, aerosol liquid water content (ALWC) enhances the nitrate uptake into particles. Field studies suggest that the increase in ALW is due to nitrate particles (Hodas et al., 2014; Wu et al., 2018). Finally, synoptic conditions can increase the

https://doi.org/10.5194/acp-2022-364
Preprint. Discussion started: 30 May 2022


Atmospheric Chemistry and Physics Discussions

concentration of nitrate particles. The high-concentration PM events in Seoul, Korea during wintertime are mainly driven by nitrate uptake, which is influenced by both the regional transport and local stagnation (Seo et al., 2020; Lim et al., 2020).

Urban areas in both China and Korea are experiencing high-concentration PM events during the wintertime. These events are characterized by inorganic-rich particles, high levels of NO_x and ammonia concentrations, low temperature, and relatively high RH leading to deliquescent particles (Huang et al., 2014; Lim et al., 2020). These conditions are ideal for nitrate particle formation. In urban areas, NO_x is easily oxidized to HNO_3 which is then partitioned into particles with NH_3 by forming NH_4NO_3. Low temperature shifts the partitioning of HNO_3-NO_3^- toward nitrate particles. Further, nitrate uptake into particles can be enhanced when particles are deliquescent and in turn, the higher the nitrate concentrations in particles, the more water vapor taken up. This "positive feedback" is thought to be the main mechanism that increases concentrations of nitrates and ALW in particles simultaneously until the system reaches thermodynamic equilibriums (Wu et al., 2018).

Therefore, thermodynamic equilibriums of inorganic species established between the gas and particle phases and also within the aqueous phase of the particles provide the key mechanisms of nitrate formation in particles (Fig. 1). Thermodynamic models (e.g., SCAPE, ISORROPIA, and E-AIM) have been developed for the computation, including the equilibrium system and the state of particles (solid vs. deliquescent) (Kim et al., 1993; Fountoukis and Nenes, 2007; Clegg et al., 1998). At a given RH and temperature, thermodynamic models can simulate the equilibrium concentrations of inorganic species in the gas and particle phase, the concentration of ALW and pH in particles. Thermodynamic models are useful for studying inorganic-rich particle formation because they provide reliable and quantitative-basis results, which can be further used for PM mitigation strategies (Li et al., 2018; Guo et al., 2018; Lim et al., 2020).

However, there are at least three associated issues which are overlooked when a thermodynamic model is used in field studies. First, the metastable mode in a thermodynamic model does not fully describe physical/chemical processes associated with water uptake and nitrate partitioning. In most cases, field studies use the metastable mode, which assumes that particles are deliquescent all over the RH range. However, this neglects the RH-dependent deliquescent behavior of inorganic particles, which are the dominant fraction of the East Asian haze. Inorganic particles are solid (dry) until the ambient RH reaches the deliquescence point of the inorganic particles, and the deliquescence RH (DRH) is not low enough to assume that the ambient RH is always above DRH. For example, ammonium-sulfate-nitrate system particles, which can be represented as the mixture of $(NH_4)_2SO_4$ and NH_4NO_3, are solid until RH reaches the deliquescence point of the mixture, RH 55% (Seinfeld and Pandis, 2016). Therefore, the "positive feedback" between nitrate and water accumulation in particles must be carefully investigated because it essentially acts as the mechanism based on the metastable-mode assumption in the equilibrium mode, and it will not work if particles are solid when the ambient RH is below DRH of the particles.

The second issue is that although the stable mode captures a deliquescence point for a single inorganic compound, it does not perform well for mixed inorganic particles. For example, the stable mode in ISORROPIA-II and E-AIM predicts very close to literature DRH values for single $(NH_4)_2SO_4$ particles and single NH_4NO_3 particles separately. However, for the mixture of

https://doi.org/10.5194/acp-2022-364
Preprint. Discussion started: 30 May 2022


Atmospheric Chemistry and Physics Discussions

$(NH_4)_2SO_4$ and NH_4NO_3, whose DRH is 55% (Seinfeld and Pandis, 2016), the stable mode in ISORROPIA and E-AIM predicts ~70% DRH, which is an average of DRHs of $(NH_4)_2SO_4$ and NH_4NO_3.

The third issue is that the organic contribution to water uptake into particles is lacking or not well expressed in a thermodynamic model. ISORROPIA does not possess an input for an organic species while E-AIM has an input for a single organic compound. However, ambient PM contains a myriad of organic components. The potential synergetic effect of organic compounds on water uptake into inorganic aerosols are also neglected. Generally, the total ALWC ($ALWC_{tot}$) is set to be the sum of the inorganic compound contribution ($ALWC_i$) and the organic contribution ($ALWC_o$) (i.e., $ALWC_{tot} = ALWC_i + ALWC_o$). Or approximately $ALWC_{tot}$ is $ALWC_i$ for inorganic-rich particles.

To overcome these issues, this work aims to determine the processes directly related to nitrate uptake, which are not clearly shown in thermodynamic model simulations, including the gas-particle partitioning of nitrates associated with RH-dependent water uptake processes. Therefore, this work will be useful not only to field studies but also to air quality models (CMAQ or GEOS-Chem) that associate with a thermodynamic model (ISORROPIA-II) by improving the real-time diurnal simulations which capture RH-dependent nitrate partitioning and water uptake at least every hour. Note that time to reach equilibriums for submicron particles is known to be within one hour (Meng and Seinfeld, 1996; Fountoukis et al., 2009; Guo et al., 2018).

In this work, we measured the hygroscopic growth factors of single/mixed inorganic particles and inorganic-organic particles using a humidified tandem differential mobility analyzer (HTDMA). Inorganic particles were generated by atomizing ammonium sulfates, ammonium nitrates or the mixture of ammonium sulfates and ammonium nitrates because ammoniums, sulfates, and nitrates were main components in East Asian haze (Lim et al., 2020). For an organic component, glyoxal was used. Glyoxal may not be the best surrogate for the atmospheric organic particles in East Asia, which contain a myriad of organic components. However, because the purpose of this study is to investigate nitrate uptake in deliquescent aerosols and a potential effect of organic components, the single organic compound would be better for determining organic contributions to nitrate and water uptake, and glyoxal is the most common water-soluble organic compounds in the atmosphere and its chemistry in the aqueous phase has been widely studied (Lim et al., 2010).

After HTDMA measurements for inorganic particles and inorganic-glyoxal particles, we compared the measurements with thermodynamic model simulations to investigate contributions of the partitioning of semivolatile ammonium nitrates to the hygroscopicity of particles. Both ISORROPIA-II and E-AIM equilibrium models are used in the stable and metastable modes. For the best-fitting to HTDMA measurements, we revised ISORROPIA-II and E-AIM simulation results and conducted linear regressions of individual simulations with the Zdanovskii Stokkes Robinson (ZSR) method, then investigated evaporation/uptake of ALWC into particles and the partitioning behavior of nitrates.

2 Methods

https://doi.org/10.5194/acp-2022-364
Preprint. Discussion started: 30 May 2022


Atmospheric Chemistry and Physics Discussions

2.1 Materials

The following chemicals were used in this work: ammonium sulfate (AS) (Sigma-Aldrich) 99.999% by weight, ammonium nitrate (AN) (Sigma-Aldrich) > 99.0% by volume, and glyoxal (Sigma-Aldrich) 40 % in H_2O by volume.

2.2 HTDMA measurement

The experimental setup is described in Fig. 2. Zero air was passed through filtered air supply (TSI 3074B) with 30 – 35 psi, then it carried inorganic or inorganic-organic aerosols generated by aerosol generator 3076, which atomized aqueous solutions of AS, AN, and glyoxal. The types of aerosols generated from the atomizer were AS, AN, the mixture of AS and AN, glyoxal, the mixture of AS and glyoxal, the mixture of AN and glyoxal, and the mixture of AS, AN, and glyoxal. The aerosols generated by the atomizer (~5000 particles/cm^3 of 250 nm-diameter dry aerosols) were passed through three dryers with the output flow rate around 3 LPM before introducing them to HTDMA. To maximize water removal, 1) two silica gel diffusion dryers (TSI 3062 NC) and one nafion dryer (Nafion^{TM} Tubing by Perma Pure) were used; 2) RH of upstream inlet was kept at 10%; and 3) a bypass filter were used to balance air pressure and to increase efficiency of drying process. HTDMA (Brechtel Model 3100A) was used to measure the hygroscopic growth factor of aerosols. HTDMA has two main units: scanning electrical mobility sizer (SEMS) and humidified scanning electrical mobility sizer (HSEMS). Each unit consists of a differential mobility analyzer (DMA) and a mixing condensation particle counter (MCPC), and they provide aerosol size distribution data. 250 nm-diameter aerosols were investigated in HTDMA because 250 nm was the average size of secondary organic aerosol (SOA) from smog chamber reactions (Lim et al., 2016). The aerosols from the atomizer were introduced to SEMS, which was maintained at 10% RH, then selected 250 nm aerosols reached the HSEM unit, where RH was adjusted between 10% and 90% to measure hygroscopic growth factors of aerosols.

2.3 Hygroscopic growth factor

In theory (Seinfeld and Pandis, 2016), hygroscopic growth factor (GF) at RH_i is defined as:

$$GF_{theory} = \frac{D_i}{D_{0\%}} \qquad (Eq. 1)$$

Here, D_i is a diameter of aerosols (i.e., wet aerosol) at RH i %, and $D_{0\%}$ is a diameter of aerosols at RH 0% (i.e., dry aerosol). Aerosols are assumed to be spherical. But in HTDMA, there is a difficulty of achieving 0 % RH. The lowest RH we could reach in SEM was 10 % RH (hence the diameter of 10% RH is $D_{10\%}$). Therefore, GF measured by HTDMA is:

$$GF_{HTDMA} = \frac{D_i}{D_{10\%}} \qquad (Eq. 2)$$

2.4 ZSR method

https://doi.org/10.5194/acp-2022-364
Preprint. Discussion started: 30 May 2022


Atmospheric Chemistry and Physics Discussions

The GFs for the mixture of inorganic aerosols, for example, AS and AN aerosols, can be viewed as the sum of those for the individual AS and AN aerosols. For the sum of individual aerosols to be directly compared with the mixture aerosols themselves, the ZSR method (Stokes and Robinson, 1966) was used to determine GF (GF_{ZSR}). Assuming the individual inorganic components in aerosols do not interact, GF_{ZSR} is given by:

$$GF_{ZSR} = \left(\sum_k \varepsilon_k GF_k{}^3\right)^{\frac{1}{3}} \qquad (Eq.3)$$

, where GF_k and ε_k are the hygroscopic growth factor and volume fraction of components k, respectively. ε_k is given by:

$$\varepsilon_k = \frac{w_k/\rho_k}{\sum_j w_j/\rho_j} \qquad (Eq.4)$$

, where w_k is the mass fraction of component k, and ρ_k is density of pure component k (Jing et al., 2016).

In this work, the ZSR method was used in two ways. First, the ZSR method was thoroughly used to calculate GF for the mixture aerosols of inorganic or inorganic-organic compounds in HTDMA measurements. For example, to estimate the GF of the mixture aerosols of AS and AN, the ZSR of individual GF_{HTDMA}(AS aerosols) and GF_{HTDMA}(AN aerosols) was estimated. Then, the ZSR estimation was compared with the HTDMA measurements for the AS-AN mixture aerosols. Second, the ZSR method was also used to estimate the GF of the mixture aerosols of inorganic and organic compounds based on output of thermodynamic model simulations.

2.5 Thermodynamic model simulation

ISORROPIA-II (Fountoukis and Nenes, 2007) and E-AIM (Clegg and Seinfeld, 2006) were used to predict concentrations of inorganic species (ammonium, ammonia, sulfate, nitric acid, and nitrate) in the gas and particle phase, ALWC of particles. In addition to inorganic species, E-AIM was used to simulate concentrations of an organic species (glyoxal). Details for thermodynamic models can be found in prior studies (Lim et al., 2020). The forward mode for ISORROPIA-II and E-AIM was used because it better constrained the simulation output and generated more realistic output than the reverse mode (Hennigan et al., 2015). Another reason for using the forward mode is that when atomized solution introduced into HTDMA, these aerosols are expected to undergoes gas-particle partitioning; therefore, concentrations of inorganic and organic compound solutions in the atomizer (input) will be the total sum of the concentrations in the gas and particle phase. In this work, hygroscopic growth factors in both the stable and metastable mode were estimated and compared with those measured by HTDMA. According to Eq. 1 and 2, two types of hygroscopic growth factors (GF(I) and GF(II)) were estimated based on output of thermodynamic model simulations. At given RH_i (temperature is 298K),

$$GF(I) = \frac{D_i}{D_{dry,i}} \qquad (Eq.7)$$

https://doi.org/10.5194/acp-2022-364
Preprint. Discussion started: 30 May 2022


Atmospheric Chemistry and Physics Discussions

, where D_i = diameter of aerosol at RH_i; $D_{dry,i}$ = diameter of water-removed aerosol (= aerosol at RH_i – ALWC at RH_i).

$$GF(II) = \frac{D_i}{D_{10\%}} \qquad (Eq. 8)$$

, where D_i = diameter of wet aerosol at RH_i; $D_{10\%}$ = diameter of wet aerosol at RH 10%.

GF(I) is the theoretical definition based on the assumption that $D_{dry,i}$ is equal to $D_{0\%}$ (Eq. 1). GF(II) is the measurement definition by our HTDMA system (Eq 2). GF(I) and GF(II) are expected to be the same because $D_{dry,\,i}$ and $D_{10\%}$ are thought to be the same. However, when the partitioning of NH_3-NH_4^+ and the partitioning of HNO_3-NO_3^- are driven by ALWC, GF(I) and GF(II) may become different. Notably, GF(I) cannot be smaller than 1, but GF(II) can. In this work both GF(I) and GF(II) were estimated to investigate the partitioning of semivolatile inorganic compounds and water uptake, and after thermodynamic model analyses GF(II) was used to fit HTDMA measurements. The thermodynamic model inputs for each aerosol sample are listed in Table S1.

3 Results and discussions

3.1 AS aerosol

The GF_{HTDMA} vs. RH plots for AS aerosols (GF_{HTDMA} = GF measured by HTDMA) are shown in Fig. S1 and S1 Text (Supplementary Material). The stable mode simulations (Fig. S1A and S2A) are consistent with past studies, which reported ~80% DRH (Aschmann et al., 1997). The hygroscopic growth factors, GF(I) and GF(II) estimated by ISORROPIA-II and E-AIM in the stable mode agree well with GF_{HTDMA} because the mass concentrations of dry AS aerosols below DRH were the same (Fig. S1A and B; Fig. S2A and B). On the contrary, the metastable mode generated ALWC in the entire RH range: ALWC increased as RH increased (Fig. S1D and S2D), and GFs(I) in both ISORROPIA-II and E-AIM simulations (i.e., ISORROPIA-II (II) and E-AIM (II)) were slightly higher than GFs(II) (ISORROPIA-II (I) and E-AIM (I)) (Fig. S1C and S2C). This is because the mass concentration of AS at RH 10% contained a small amount of ALWC, and was not completely dry (Fig. S1D and S2D).

3.2 AN aerosol

Our HTDMA results for AN aerosols showed no distinctive deliquescence point, rather smooth rising curves (Fig. 3; Fig. S3A and D; Fig. S4A and D), which indicate the water uptake into aerosols in the entire RH range (Fig. S3F and S4F). This differs from what we commonly know: AN aerosols are solid until RH reaches a deliquescence point at ~60% RH (Seinfeld and Pandis, 2016). This deliquescent behavior of AN aerosols is described by the stable-mode simulation curve from both ISORROPIA-II and E-AIM (Fig. S3A and S4A) with the absence of ALWC below DRH. (Fig. S3C and S4C) Above DRH in the stable-mode curves, GF(II) became slightly greater than GF(I) (Fig. S3A and S4A). This is because $D_{dry,i}$ is greater

https://doi.org/10.5194/acp-2022-364
Preprint. Discussion started: 30 May 2022


Atmospheric Chemistry and Physics Discussions

than $D_{10\%}$ above DRH (Fig. S3C and S4C). Once aerosols become deliquescent, ALWC takes up more ammoniums and nitrates by shifting the partitioning of NH_3-NH_4^+ and NO_3-HNO_3 toward particles.

A number of groups have reported that AN aerosols possess a similar smooth rising curve (Svenningsson et al., 2006; Hu et al., 2011). AN aerosols are deliquescent all over RH as removing water completely from AN aerosols is extremely difficult. ISORROPIA-II Metastable (I) and E-AIM Metastable (I) simulated growth factors close to HTDMA measurements; however, ISORROPIA-II Metastable (II) and E-AIM Metastable (II) were significantly different from the HTDMA measurements and their simulation results are also different from each other (Fig. S3D and S4D). ISORROPIA-II Metastable simulates that ammonia and nitric acid were almost ~100% partitioned into particles at RH 10% ($[NH_4^+]$ = 10 μg/m^3 and $[NO_3^-]$ = 40 μg/m^3) and as RH increased, and the evaporation occurred until RH 30% at which 22 μg/m^3 of nitrate particles remained (Fig. S3E and F) (Note that this level of nitrates is what the stable mode predicts below DRH 65% (Fig S3B)). Above RH 30% ammonium nitrate aerosols take up water vapors and more ammonium nitrates are accumulated into particles (Fig. S3F). Unlike ISORROPIA-II simulations, E-AIM in the metastable mode predicted only 12 μg/m^3 of nitrates at RH 10% while 23 μg/m^3 of nitrates was predicted in the stable mode (Fig. S4E). As RH increased, more ammonium nitrates and ALWC were accumulated (Fig. S4F).

Neither the stable mode nor the metastable mode simulations by thermodynamic models agreed with HTDMA measurements. In particular, the metastable mode simulations for nitrates at RH 10% were unrealistic: ISORROPIA-II overestimated and E-AIM underestimated. Therefore, we introduced $AN_{ISO\_CORRECTION}$ and $AN_{EAIM\text{-}CORRECTION}$, which were revised GF curves for AN aerosols by fitting to HTDMA measurements in Fig. 3 and Fig. S5, respectively (Details are described in S1 Text). $AN_{ISO\text{-}CORRECTION}$ and $AN_{EAIM\text{-}CORRECTION}$ were used as an AN aerosol reference in the following sections to investigate thermodynamic equilibriums for the mixture of AS and AN aerosols, and the mixture of AS, AN and glyoxal aerosols. We found two simulations based on ISORROPIA-II and E-AIM very close each other for the mixture aerosols in the following sections. To avoid duplication, ISORROPIA-II simulation results are given in the main text and corresponding E-AIM simulation results are provided in Supplementary Material.

3.3 Mixture of AS and AN aerosol

3.3.1 AS : AN = 80 : 20

GFs based on HTDMA measurements (HTDMA) did not agree with GFs estimated by the sum of HTDMA measurements of individual AS and AN aerosols with the ZSR method (ZSR($0.8AS_{HTDMA}$ + $0.2\ AN_{HTDMA}$)) (Fig. 4A). In the range of RH 30% to 70% of Fig. 4A, the HTDMA measurement was significantly lower than ZSR($0.8AS_{HTDMA}$ + $0.2AN_{HTDMA}$). Here, we attempted to prove that the overestimation of ZSR($0.8AS_{HTDMA}$ + $0.2AN_{HTDMA}$) must be due to the evaporation of aerosol components. Since none of ISORROPIA-II and E-AIM simulations in the stable mode and metastable mode for mixture of AS and AN aerosols agreed with HTDMA measurements (Fig. S6 and S7), we introduced ISORROPIA-II CORRECTION 1

https://doi.org/10.5194/acp-2022-364
Preprint. Discussion started: 30 May 2022


Atmospheric Chemistry and Physics Discussions

(Fig. 4A), which is the linear regression of the revised stable-mode simulations for AS aerosols (Table S2) and $AN_{ISO\_CORRECTION}$ (Fig. 3A). Similarly, E-AIM CORRECTION 1 (Fig. S8) is the linear regression of the revised stable-mode simulations for AS aerosols (Table S2) and $AN_{E\text{-}AIM\_CORRECTION}$ (Fig. S5A). Note that the stable-mode for AS aerosols was modified to simulate ALWC in the RH range 55% to 80% because DRH for the mixture of AS and AN aerosols was 55% (Table S2), and the ALWC values were based on the metastable mode simulations in the corresponding RH.

ISORROPIA-II CORRECTION 1 overestimated GF (Fig. 4A), so ISORROPIA-II CORRECTION 2 was performed by removing ALWC from ISORROPIA-II CORRECTION 1 (Fig. 4F). Although ISORROPIA-II CORRECTION 2 in Fig. 4D was further reduced, it was still slightly overestimated. Thus, ISORROPIA-II CORRECTION 3 was performed by removing remained nitrates and ammoniums in aerosols (Fig. 4I) then it was finally fitted to HTDMA measurements (Fig. 4G). Substantial evaporation of ALWC, nitrates and ammoniums can be attributed to the large fraction of AS aerosols, which tend to remain solid as ammonium sulfate crystals below DRH 80%. Indeed, in the RH range of 45 to 55% all nitrates completely evaporated and the mixture existed as dry ammonium sulfate crystals (Fig. 4I). The same results were obtained in E-AIM simulations (Fig. S8).

3.3.2 AS : AN = 50 : 50

HTDMA measurements showed a DRH point at 55% and the measurement data are consistent with existing literature (Fig. 5 and S9) (Seinfeld and Pandis, 2016). With the comparison of $ZSR(0.5AS_{HTDMA} + 0.5AN_{HTDMA})$, HTDMA measurements were slightly lower in the RH range of 10 to 55% and much higher in the RH range of 55 to 80% and similar above RH 80% (Fig. 5A and D; Fig. S9A and D). We performed the same correction as we did for AS : AN (80 : 20) to fit ISORROPIA-II CORRECTION 2 simulations to HTMDA measurements. While aerosols could be considered to be dry as solid ammonium-sulfate-nitrate crystals below RH 55%, our simulations showed the partial evaporation of ALWC, nitrates and ammoniums; therefore, the aerosols should be still deliquescent (Fig. 5F and S9F). To prove this, we needed to show that ALWC should exist at RH 10%. When we adjusted $AN_{NEW\_ISO\_CORRECTION}$ to be dry at RH 10% and to follow the metastable trend as RH increase (Fig. S10A), the new fitting (ISOROPIA-II CORRECTION 2) predicted no ALWC present below RH 50% (Fig. S10D and F). However, this new fitting (ISORROPIA-II CORRECTION 3) overestimated GF for the mixture of AS and AN aerosols (80 : 20) even after complete evaporation of ALWC, nitrates and ammoniums between RH 30% and RH 65% (Fig. S10G and I). For the best-fitting to HTDMA measurements, mass concentrations at RH 10% must be larger by containing ALWC. Furthermore, a previous laboratory study reported that RH-dependent evaporation required a hydrated form (Hu et al., 2011; Hightower and Richardson, 1988) (i.e., the gas-particle partitioning of $HNO_3{\cdot}nH_2O\text{-}NO_3^-$ and $NH_3{\cdot}nH_2O\text{-}NH_4^+$, instead of the gas-particle partitioning of $HNO_3\text{-}NO_3^-$ and $NH_3\text{-}NH_4^+$) when evaporation of aerosol components occurs with an increase in RH.

3.3.3 AS : AN = 20 : 80

https://doi.org/10.5194/acp-2022-364
Preprint. Discussion started: 30 May 2022


Atmospheric Chemistry and Physics Discussions

Similarly to the mixtures of AS and AN aerosols (80 : 20 and 50 : 50), the mixture of AS and AN aerosols with the ratio of 20 : 80, respectively, requires evaporation of ALWC, nitrates and ammoniums to be fitted to HTDMA measurements (Fig. 6D and F; Fig. S11D and F). Again, this mixture aerosols were deliquescent in the entire RH range (Fig. 6F). Overall, fitting E-AIM simulations to HTDMA measurements for the all mixtures of AS and AN aerosols also exhibited the same results (refers to: 3.3.1 and 3.3.2) (Fig. S8, S9 and S11).

3.4 Mixture of inorganic and glyoxal aerosol

3.4.1 Glyoxal aerosol (GLY aerosol)

According to HTDMA measurements, GF of glyoxal aerosols (GLY_{HTDMA}) had a smooth rising curve as RH increases (Fig. S12A). In this case, GLY_{MODEL}, the fitting, can be expressed as an equation form with RH dependence:

$$GLY_{MODEL} = \left[1 + (0.3362 - 0.1513 \times RH + 0.1022 \times RH^2)\frac{RH}{1 - RH}\right]^{1/3} \quad (Eq. 9)$$

Although E-AIM allows input for organic compounds, none of E-AIM simulations agreed with GLY_{HTDMA} (Fig. S12A) and mixtures of AS-glyoxal and AN-glyoxal aerosols (Fig. S12B, C, and D). Thus, in this work, the GLY_{MODEL} was thoroughly used for fitting to mixtures of inorganic and glyoxal aerosols.

3.4.2 AS-GLY mixed aerosols

ISORROPIA-II CORRECTION 1 was obtained by the linear regression of $AS_{ISORROPIA\text{-}II\ Stable}$ (Fig. S1) and GLY_{MODEL} (Fig. S12A) with ZSR method and the ratio of AS and GLY. In Fig. 7A (AS : GLY = 70 : 30), only glyoxal contributed to ALWC formation in the RH range of 10-60%; however, the range of 60-80% RH exhibited a strong synergetic effect on ALWC formation (Fig. 7D). For the best-fitting, ISORROPIA-II CORRECTION 2 was constructed by adding ALWC in the range of 55 to 80% RH.

For AS : GLY (50 : 50), a synergetic effect on ALWC formation was observed in the entire RH range (Fig. 7B). For the best-fitting, ISORROPIA-II CORRECTION 2 was constructed by adding ALWC in the range of 10 to 60% RH besides the range of 60 to 80% RH (Fig. 7E). The same results were obtained in E-AIM simulations (Fig. S13A, B, D and E).

3.4.3 AN-GLY mixed aerosols

In Fig. 7C, ISORROPIA-II CORRECTION 1 is obtained by the sum of $AN_{ISO\_CORRECTION}$ (Fig. 3A) and GLY_{MODEL} with ZSR method and the ratio of (50 : 50). Below RH 80%, ISORROPIA-II CORRECTION 1 agreed well with HTDMA measurements. E-AIM CORRECTION 1 also agreed well with HTDMA measurements (Fig. S13C). There was no synergetic effect below 80% RH; therefore, total ALWC was the sum of the individual contributions of AN and glyoxal aerosols.

https://doi.org/10.5194/acp-2022-364
Preprint. Discussion started: 30 May 2022


Atmospheric Chemistry and Physics Discussions

3.4.4 AS-AN-GLY mixed aerosols

The mixture of AS, AN, and GLY aerosols with the ratio of 50 : 50 : 20, respectively, was prepared to mimic ambient $PM_{2.5}$ during the high-concentration event at Seoul, Korea (February 24-28, 2014) by having the similar ratio of particle components. Based on our thermodynamic simulations, our mixture aerosols contained 20% ammoniums, 31% sulfates, 29% nitrates, and 19% organics at RH 60% while in PM2.5 during the high-concentration event at Seoul, 18% ammoniums, 29% sulfates, 27% nitrates and 22% organic matter at average RH 59% were measured. Note that those fractions are mass basis.

ISORROPIA-II CORRECTION 1 is the sum of $AS_{ISORROPIA\text{-}II\ Stable\ Revised}$ (Table S2), $AN_{ISO\_CORRECTION}$ (Fig. 3A) and GLY_{MODEL} (Fig. S12A) with the ZSR method and the corresponding ratio of AS, AN and GLY aerosols. The simulation of ISORROPIA-II CORRECTION 1 is very close to HTDMA measurements (Fig. 8A). It appears that no synergetic effect exists for glyoxal in inorganic aerosols on ALWC formation. In the range of 10-50% RH, ISORROPIA-II CORRECTION 1 slightly overestimates HTDMA measurements. This is due to the evaporation of ALWC, nitrates and ammoniums as observed in inorganic mixture aerosols. In the range of 50 to 80% RH, the HTDMA measurements and ISORROPIA-II CORRECTION 1 were greater than $ZSR(0.5AS_{HTDMA} + 0.5AN_{HTDMA} + 0.2GLY_{HTDMA})$ because of the synergetic effect of AS and AN aerosols on ALWC formation in the same RH range. Again, the same results were obtained in E-AIM simulations (Fig. S14).

3.5 Limitations

This work focuses on fitting our revised thermodynamic model simulations ($GF_{ISO\_CORRECTION}$ and $GF_{E\text{-}AIM\_CORRECTION}$) to the HTDMA measurements and discussing the uptake and evaporation of ALWC, nitrates and ammoniums. Therefore, limitations in this work are uncertainties of molecular-level interactions among inorganic ions, organic compounds, and water (e.g., solvent-ion effects) that affect thermodynamic equilibriums. A detailed study of particle morphology including solid/liquid-like phase, phase separation or evenly distributed mixture as a bulk, and potential condensed phase chemistry would provide better understanding of thermodynamic equilibriums in hygroscopic particles. This study of particle morphology is beyond the scope of this work. Here we focused on nitrate and water uptake interpreted by HTDMA measurements and thermodynamic model analyses.

Notably in this study we assume that ALWC still exists in inorganic particles below DRH to achieve the best-fitting to HTDMA measurements. The existence of ALWC due to incomplete equilibriums of AN aerosols warrants further investigation (i.e., solvation effect of nitrates) as the existence of ALWC itself has been commonly observed while conditioning filter samples of ambient aerosols (Kajino et al., 2006).

4 Conclusions and atmospheric implications

https://doi.org/10.5194/acp-2022-364
Preprint. Discussion started: 30 May 2022


Atmospheric Chemistry and Physics Discussions

In ambient conditions, particles of the ammonium-sulfate-nitrate system with significant nitrates are deliquescent even at low RH because the particles undergo hysteresis with an unclear efflorescent RH point due to incomplete equilibriums, thus the complete evaporation of ALWC from AN aerosols is extremely difficult. Due to the deliquescent nature, the metastable mode is more appropriate than the stable mode for most ambient condition simulations. However, the growth factor estimated by the metastable mode may have an uncertainty because $D_{dry\ i}$ is not the same in the entire RH range (i.e., GF(I) and GF(II) are different) and the metastable mode does not capture the evaporation of ALWC, nitrates, and ammoniums as RH increases. When the fraction of nitrates is small, particles of the ammonium-sulfate-nitrate system will become dry ammonium sulfate aerosols in the RH range of 30 to 70% by evaporating ALWC, nitrates and ammoniums significantly. Glyoxal contributes to ALWC formation by adding its own hygroscopicity to the ammonium-sulfate-nitrate system particles (i.e., $ALWC_{tot} = ALWC_{inorganic} + ALWC_{gly}$) in the entire range of RH. Above ~50% RH a synergetic ALWC formation takes place with the ammonium-sulfate-nitrate system particles and the closer observation indicates that the synergetic effect on ALWC formation actually takes place between AS and AN aerosols and the effect of glyoxal is negligible.

The positive feedback between ALWC and nitrate formation until equilibriums is thought to be the main mechanism of massive nitrate formation during haze events in East Asia at relatively high RH. But when RH is modest (below RH 50%), the positive feedback will be driven by deliquescent nature of ammonium nitrates. Furthermore, the positive feedback must overcome a barrier created by ammonium sulfate aerosols that suppress ALWC and nitrate accumulation in the RH range of 30 to 70%. Therefore, the positive feedback will reinforce the uptake of HNO_3 during the nighttime, whose RH is likely to be higher with significant HNO_3 formation through heterogeneous reactions of N_2O_5 (Liu et al., 2020). Once nitrates are accumulated in ammonium sulfate particles, the uptake of HNO_3 photochemically formed during the daytime, whose RH is likely to be lower, may be of importance.

Synergetic effects of organic compounds on hygroscopicity of inorganic particles are a critical subject that warrants future studies. As we observed in the case of glyoxal with AS aerosols at high RH, there exists a synergetic effect of glyoxal with sulfates on ALWC formation. Sulfates greatly increase the water solubility of glyoxal through solvent-ion effects and form organosulfates (Lim et al., 2010). As the formation of organosulfates affects equilibrium in the aqueous phase and between the gas and particle phase, we cannot rule out the possibility of organosulfates effecting hygroscopicity. OH-radical reactions are the main sink for glyoxal in the aqueous phase (Lim et al., 2010). Abundance of nitrates in particles may act as a source of OH radicals (Zhang et al., 2022), and the increase in O/C of organic products may enhance the hygroscopicity (Jimenez et al., 2009). Finally, good agreements between field measurements and metastable-mode simulation outputs for inorganic-rich particles in East Asia suggest that synergetic effects work for the entire RH range (Lim et al., 2020), whereas glyoxal only works for ammonium sulfate aerosols above ~50% RH. A recent study also reports that the contribution of organics on ALWC formation is significant in East Asia (Jin et al., 2020). Effects of secondary organic aerosol (SOA) on thermodynamic equilibriums leading to hygroscopicity of particles may be the greatest uncertainty.

https://doi.org/10.5194/acp-2022-364
Preprint. Discussion started: 30 May 2022


Atmospheric Chemistry and Physics Discussions

Author contribution

HDD and YBL conceptualized the project. YBL supervised the project. HDD conducted experiments and analyzed HTDMA data. HDD and YBL conducted and analyzed thermodynamic model simulations. HDD prepared data, and wrote the draft. YBL wrote and edited the manuscript. YPK validated thermodynamic model results, reviewed and edited the manuscript.

Competing interest

The authors declare that they have no known competing financial interests or personal relationships that could have appeared to influence the work reported in this paper.

Acknowledgments

This work is supported by Fine Particle Research Initiative in East Asia Considering National Differences (FRIEND) Project through NRF funded by Ministry of Science and ICT (2020M3G1A1114558), Basic Science Research Program through NRF funded by Ministry of Education (2021R1I1A1A01059748) in South Korea. Authors thank Fred Brechtel for helpful discussions.

Supplement

Supplementary material contains S1 Text, Table S1-S2 and Figures S1–S14.

https://doi.org/10.5194/acp-2022-364
Preprint. Discussion started: 30 May 2022

Atmospheric Chemistry and Physics Discussions

References

Aschmann, S. M., Chew, A. A., Arey, J., and Atkinson, R.: Products of the Gas-Phase Reaction of OH Radicals with Cyclohexane: Reactions of the Cyclohexoxy Radical, The Journal of Physical Chemistry A, 101, 8042-8048, 10.1021/jp971869f, 1997.

Clegg, S. L. and Seinfeld, J. H.: Thermodynamic Models of Aqueous Solutions Containing Inorganic Electrolytes and Dicarboxylic Acids at 298.15 K. 1. The Acids as Nondissociating Components, The Journal of Physical Chemistry A, 110, 5692-5717, 10.1021/jp056149k, 2006.

Clegg, S. L., Brimblecombe, P., and Wexler, A. S.: Thermodynamic Model of the System H^+–NH_4^+–Na^+–SO_4^{2-}–NO_3^-–Cl^-–H_2O at 298.15 K, The Journal of Physical Chemistry A, 102, 2155-2171, 10.1021/jp973043j, 1998.

Fountoukis, C. and Nenes, A.: ISORROPIA II: a computationally efficient thermodynamic equilibrium model for K^+-Ca^{2+}-Mg^{2+}-NH_4^+-Na^+-SO_4^{2-}-NO_3^--Cl^--H_2O aerosols, Atmos. Chem. Phys., 7, 4639-4659, 10.5194/acp-7-4639-2007, 2007.

Fountoukis, C., Nenes, A., Sullivan, A., Weber, R., Van Reken, T., Fischer, M., Matías, E., Moya, M., Farmer, D., and Cohen, R. C.: Thermodynamic characterization of Mexico City aerosol during MILAGRO 2006, Atmos. Chem. Phys., 9, 2141-2156, 10.5194/acp-9-2141-2009, 2009.

Guo, H., Otjes, R., Schlag, P., Kiendler-Scharr, A., Nenes, A., and Weber, R. J.: Effectiveness of ammonia reduction on control of fine particle nitrate, Atmos. Chem. Phys., 18, 12241-12256, 10.5194/acp-18-12241-2018, 2018.

Hennigan, C. J., Izumi, J., Sullivan, A. P., Weber, R. J., and Nenes, A.: A critical evaluation of proxy methods used to estimate the acidity of atmospheric particles, Atmos. Chem. Phys., 15, 2775-2790, 10.5194/acp-15-2775-2015, 2015.

Hightower, R. L. and Richardson, C. B.: Evaporation of ammonium nitrate particles containing ammonium sulfate, Atmospheric Environment 22, 2587-2591, https://doi.org/10.1016/0004-6981(88)90492-1, 1988.

Hodas, N., Sullivan, A. P., Skog, K., Keutsch, F. N., Collett, J. L., Decesari, S., Facchini, M. C., Carlton, A. G., Laaksonen, A., and Turpin, B. J.: Aerosol Liquid Water Driven by Anthropogenic Nitrate: Implications for Lifetimes of Water-Soluble Organic Gases and Potential for Secondary Organic Aerosol Formation, Environmental Science & Technology, 48, 11127-11136, 10.1021/es5025096, 2014.

Hu, D., Chen, J., Ye, X., Li, L., and Yang, X.: Hygroscopicity and evaporation of ammonium chloride and ammonium nitrate: Relative humidity and size effects on the growth factor, Atmos Environ, 45, 2349-2355, http://dx.doi.org/10.1016/j.atmosenv.2011.02.024, 2011.

Huang, R.-J., Zhang, Y., Bozzetti, C., Ho, K.-F., Cao, J.-J., Han, Y., Daellenbach, K. R., Slowik, J. G., Platt, S. M., Canonaco, F., Zotter, P., Wolf, R., Pieber, S. M., Bruns, E. A., Crippa, M., Ciarelli, G., Piazzalunga, A., Schwikowski, M., Abbaszade, G., Schnelle-Kreis, J., Zimmermann, R., An, Z., Szidat, S., Baltensperger, U., Haddad, I. E., and Prevot, A. S. H.: High secondary aerosol contribution to particulate pollution during haze events in China, Nature, 514, 218-222, 10.1038/nature13774, 2014.

Jimenez, J. L., Canagaratna, M. R., Donahue, N. M., Prevot, A. S. H., Zhang, Q., Kroll, J. H., DeCarlo, P. F., Allan, J. D., Coe, H., Ng, N. L., Aiken, A. C., Docherty, K. S., Ulbrich, I. M., Grieshop, A. P., Robinson, A. L., Duplissy, J., Smith, J. D., Wilson, K. R., Lanz, V. A., Hueglin, C., Sun, Y. L., Tian, J., Laaksonen, A., Raatikainen, T., Rautiainen, J., Vaattovaara, P., Ehn, M., Kulmala, M., Tomlinson, J. M., Collins, D. R., Cubison, M. J., Dunlea, E. J., Huffman, J. A., Onasch, T. B., Alfarra, M. R., Williams, P. I., Bower, K., Kondo, Y., Schneider, J., Drewnick, F., Borrmann, S., Weimer, S., Demerjian, K., Salcedo, D., Cottrell, L., Griffin, R., Takami, A., Miyoshi, T., Hatakeyama, S., Shimono, A., Sun, J. Y., Zhang, Y. M., Dzepina, K., Kimmel, J. R., Sueper, D., Jayne, J. T., Herndon, S. C., Trimborn, A. M., Williams, L. R., Wood, E. C., Middlebrook, A. M., Kolb, C. E., Baltensperger, U., and Worsnop, D. R.: Evolution of Organic Aerosols in the Atmosphere, Science, 326, 1525-1529, 10.1126/science.1180353, 2009.

Jin, X., Wang, Y., Li, Z., Zhang, F., Xu, W., Sun, Y., Fan, X., Chen, G., Wu, H., Ren, J., Wang, Q., and Cribb, M.: Significant contribution of organics to aerosol liquid water content in winter in Beijing, China, Atmos. Chem. Phys., 20, 901-914, 10.5194/acp-20-901-2020, 2020.

Jing, B., Tong, S., Liu, Q., Li, K., Wang, W., Zhang, Y., and Ge, M.: Hygroscopic behavior of multicomponent organic aerosols and their internal mixtures with ammonium sulfate, Atmos. Chem. Phys., 16, 4101-4118, 10.5194/acp-16-4101-2016, 2016.

Kajino, M., Winiwarter, W., and Ueda, H.: Modeling retained water content in measured aerosol mass, Atmos Environ, 40, 5202-5213, https://doi.org/10.1016/j.atmosenv.2006.04.016, 2006.

Kim, Y. P., Seinfeld, J. H., and Saxena, P.: Atmospheric Gas-Aerosol Equilibrium I. Thermodynamic Model, Aerosol Science and Technology, 19, 157-181, 10.1080/02786829308959628, 1993.

Li, H., Zhang, Q., Zheng, B., Chen, C., Wu, N., Guo, H., Zhang, Y., Zheng, Y., Li, X., and He, K.: Nitrate-driven urban haze pollution during summertime over the North China Plain, Atmos. Chem. Phys., 18, 5293-5306, 10.5194/acp-18-5293-2018, 2018.

Lim, Y. B., Kim, H., Kim, J. Y., and Turpin, B. J.: Photochemical organonitrate formation in wet aerosols, Atmos. Chem. Phys., 16, 12631-12647, 10.5194/acp-16-12631-2016, 2016.

Lim, Y. B., Seo, J., Kim, J. Y., Kim, Y. P., and Jin, H. C.: Local formation of sulfates contributes to the urban haze with regional transport origin, Environmental Research Letters, 15, 084034, 10.1088/1748-9326/ab83aa, 2020.

Lim, Y. B., Tan, Y., Perri, M. J., Seitzinger, S. P., and Turpin, B. J.: Aqueous chemistry and its role in secondary organic aerosol (SOA) formation, Atmospheric Chemistry and Physics, 10, 10521-10539, 10.5194/acp-10-10521-2010, 2010.

Liu, L., Bei, N., Hu, B., Wu, J., Liu, S., Li, X., Wang, R., Liu, Z., Shen, Z., and Li, G.: Wintertime nitrate formation pathways in the north China plain: Importance of N2O5 heterogeneous hydrolysis, Environmental Pollution, 266, 115287, https://doi.org/10.1016/j.envpol.2020.115287, 2020.

Meng, Z. and Seinfeld, J. H.: Time scales to achieve atmospheric gas-aerosol equilibrium for volatile species, Atmos Environ, 30, 2889-2900, https://doi.org/10.1016/1352-2310(95)00493-9, 1996.

https://doi.org/10.5194/acp-2022-364
Preprint. Discussion started: 30 May 2022

Seinfeld, J. H. and Pandis, S. N.: Atmospheric chemistry and physics: from air pollution to climate change, 3rd, John Wiley & Sons, 1152 pp.2016.

Seo, J., Lim, Y. B., Youn, D., Kim, J. Y., and Jin, H. C.: Synergistic enhancement of urban haze by nitrate uptake into transported hygroscopic particles in the Asian continental outflow, Atmos. Chem. Phys., 20, 7575-7594, 10.5194/acp-20-7575-2020, 2020.

Stokes, R. and Robinson, R.: Interactions in aqueous nonelectrolyte solutions. I. Solute-solvent equilibria, The Journal of Physical Chemistry, 70, 2126-2131, 1966.

Svenningsson, B., Rissler, J., Swietlicki, E., Mircea, M., Bilde, M., Facchini, M. C., Decesari, S., Fuzzi, S., Zhou, J., Mønster, J., and Rosenørn, T.: Hygroscopic growth and critical supersaturations for mixed aerosol particles of inorganic and organic compounds of atmospheric relevance, Atmos. Chem. Phys., 6, 1937-1952, 10.5194/acp-6-1937-2006, 2006.

Wu, Z., Wang, Y., Tan, T., Zhu, Y., Li, M., Shang, D., Wang, H., Lu, K., Guo, S., Zeng, L., and Zhang, Y.: Aerosol Liquid Water Driven by Anthropogenic Inorganic Salts: Implying Its Key Role in Haze Formation over the North China Plain, Environmental Science & Technology Letters, 5, 160-166, 10.1021/acs.estlett.8b00021, 2018.

Zhang, R., Gen, M., Liang, Z., Li, Y. J., and Chan, C. K.: Photochemical Reactions of Glyoxal during Particulate Ammonium Nitrate Photolysis: Brown Carbon Formation, Enhanced Glyoxal Decay, and Organic Phase Formation, Environmental Science & Technology, 56, 1605-1614, 10.1021/acs.est.1c07211, 2022.

https://doi.org/10.5194/acp-2022-364
Preprint. Discussion started: 30 May 2022

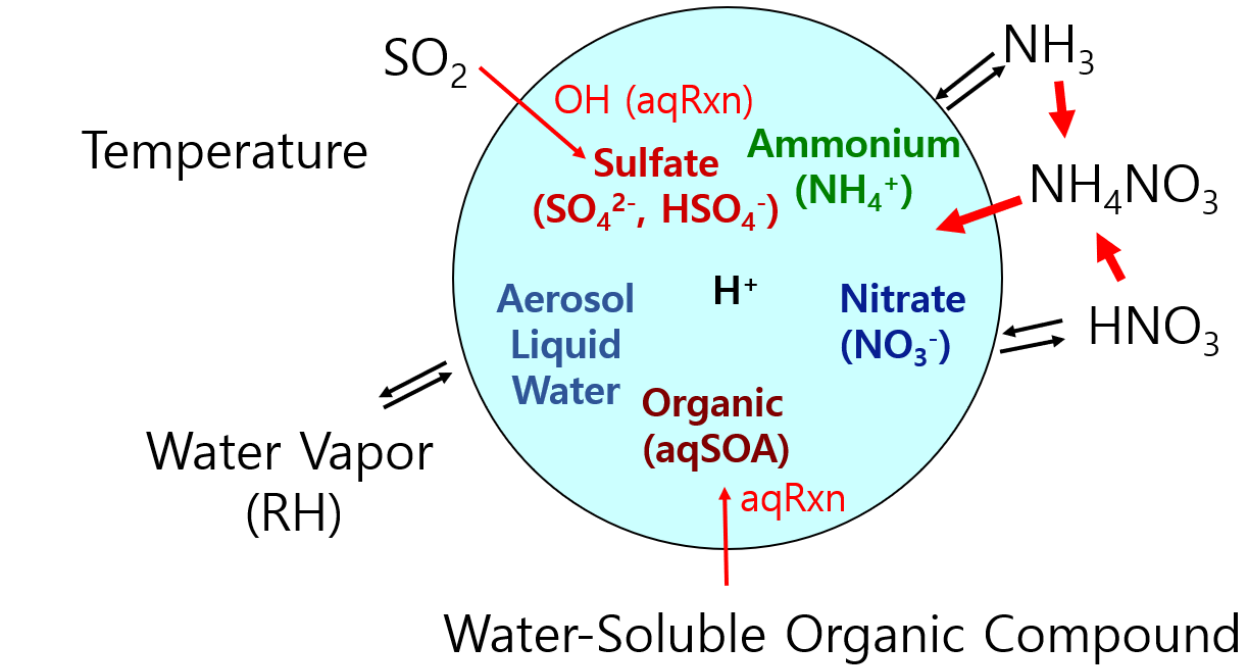

Figure 1: Thermodynamic equilibrium system. Equilibriums of inorganic species are established between the gas and (aqueous) particle phase ($HNO_{3(g)}$-$NO_{3(p)}$, $NH_{3(g)}$-$NH_4^+{}_{(p)}$, and in the aqueous phase (NH_4^+, SO_4^{2-}, HSO_4^-, NO_3^-, and H^+). The partitioning of $HNO_{3(g)}$-$NO_{3(p)}$ and $NH_{3(g)}$-$NH_4^+{}_{(p)}$ can be viewed as the formation of ammonium nitrates$_{(p)}$ by the reaction of ammonia and nitric acid in the gas phase. Sulfates are dominantly formed via aqueous-phase reaction of SO_2 with OH. Organic represents aqueous-phase secondary organic aerosol (aqSOA), which is formed via aqueous-phase reactions (aqRxn) of dissolved water-soluble organic compounds. The light blue color in the circle represents that particles are deliquescent.

https://doi.org/10.5194/acp-2022-364
Preprint. Discussion started: 30 May 2022

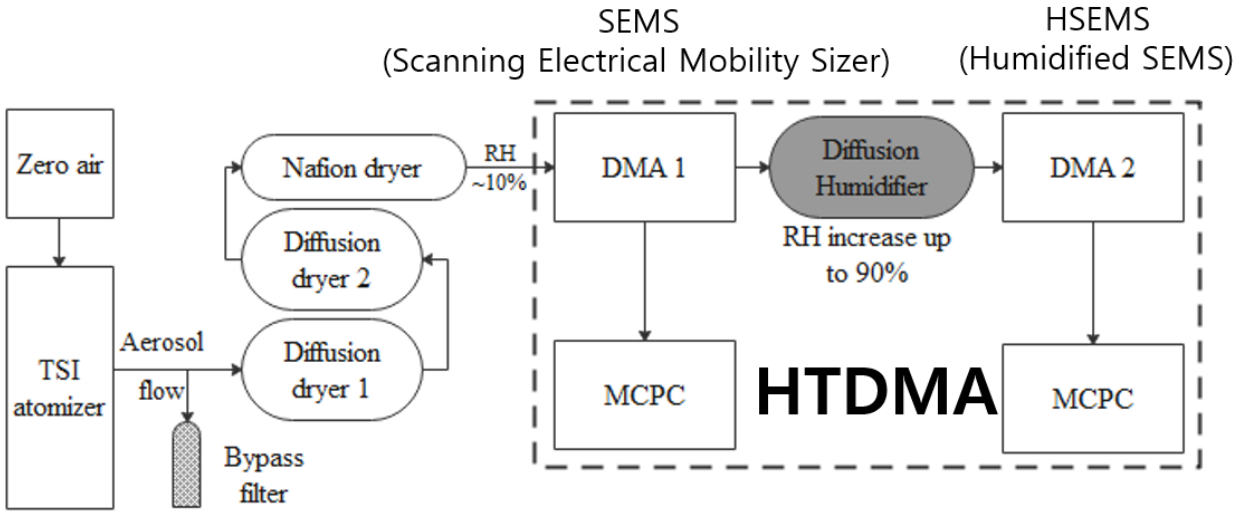

Figure 2: Experimental setup for particle's hygroscopicity analysis using a hygroscopic tandem mobility analyzer (HTDMA). DMA represents a differential mobility analyzer. MCPC represents a mixing condensation particle counter.

https://doi.org/10.5194/acp-2022-364
Preprint. Discussion started: 30 May 2022

Atmospheric Chemistry and Physics Discussions

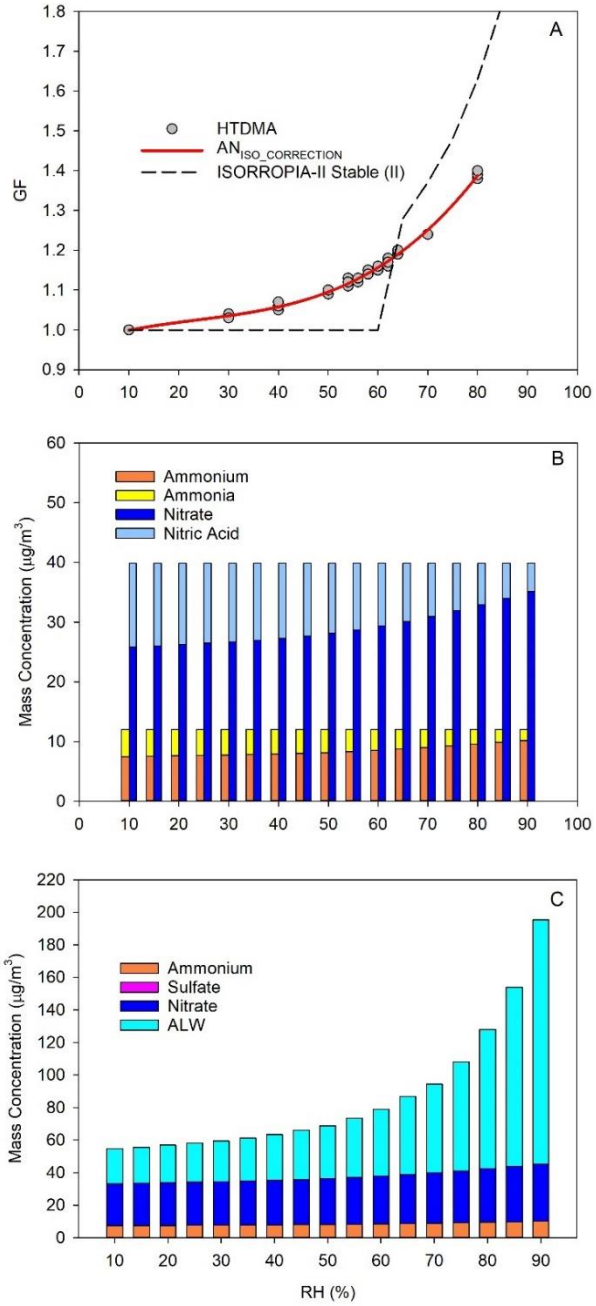

Figure 3: Hygroscopic growth factor (GF) vs. RH plots for AN aerosols. HTDMA indicates measurements by HTDMA. $AN_{ISO\_CORRECTION}$ indicates GF of AN aerosols obtained by the linear regression (S2 Text). Ammonium, Sulfate, Nitrate, and ALW are in the particle phase. Ammonia and Nitric Acid are in the gas phase. Their simulation results based on $AN_{ISO\_CORRECTION}$ are plotted with RH in (B) and (C).

https://doi.org/10.5194/acp-2022-364
Preprint. Discussion started: 30 May 2022

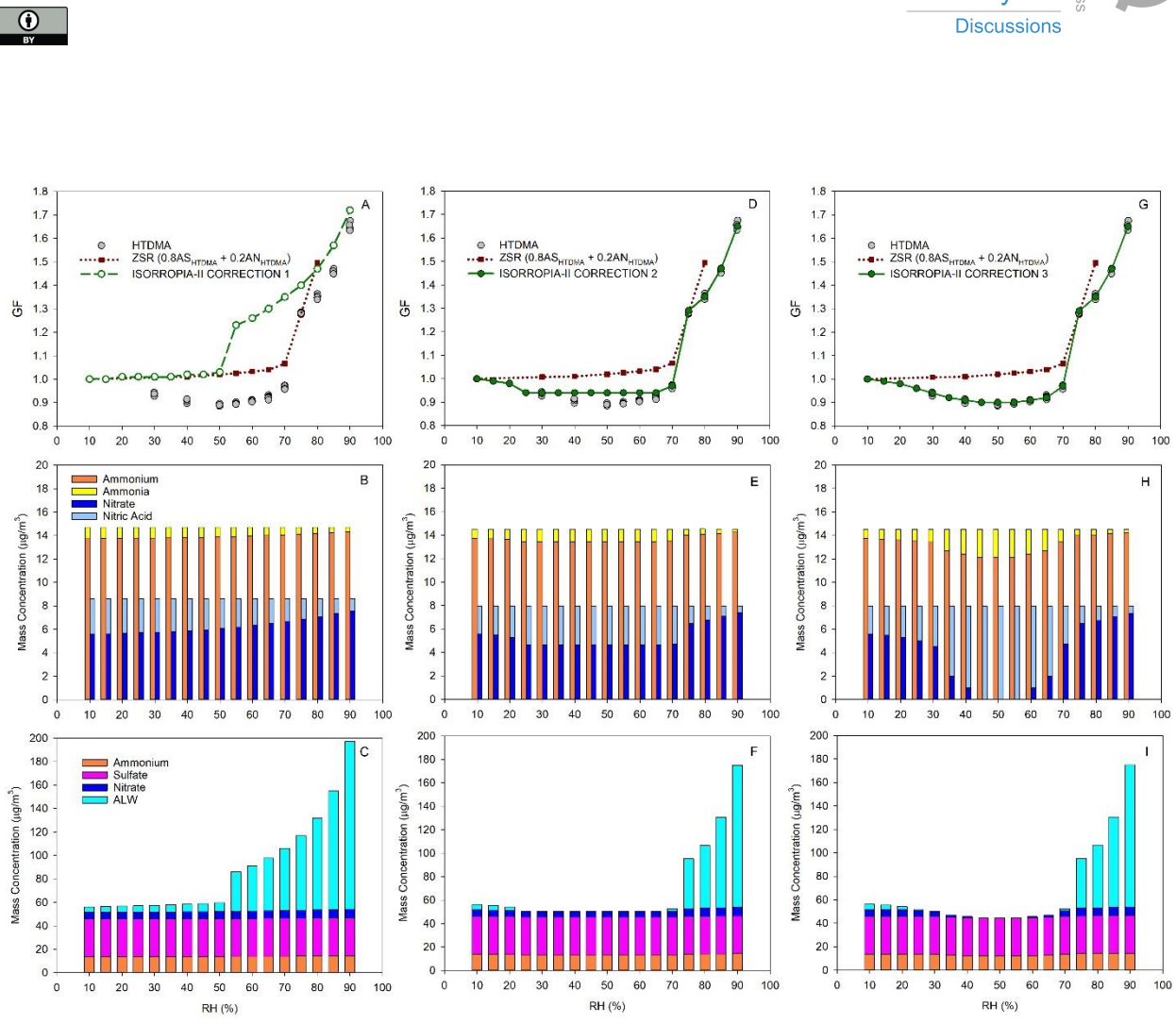

Figure 4: GF vs. RH plots for the mixture aerosols with the mass-based ratios of ammonium sulfates and ammonium nitrates to be 80 : 20 (A, D, and G). ZSR(0.8AS$_{HTDMA}$ + 0.2AN$_{HTDMA}$) indicates the sum of HTDMA measurements for individual AS aerosols and AN aerosols with ZSR method (AS : AN = 80 : 20). The gas-particle partitioning of ammonium$_{(p)}$-ammonia$_{(g)}$ and nitrate$_{(p)}$-nitric acid$_{(g)}$ (B, E, and G). The mass concentrations of ammoniums, sulfates, nitrates and ALW in the mixture aerosols vs. RH (C, F, I).

https://doi.org/10.5194/acp-2022-364
Preprint. Discussion started: 30 May 2022

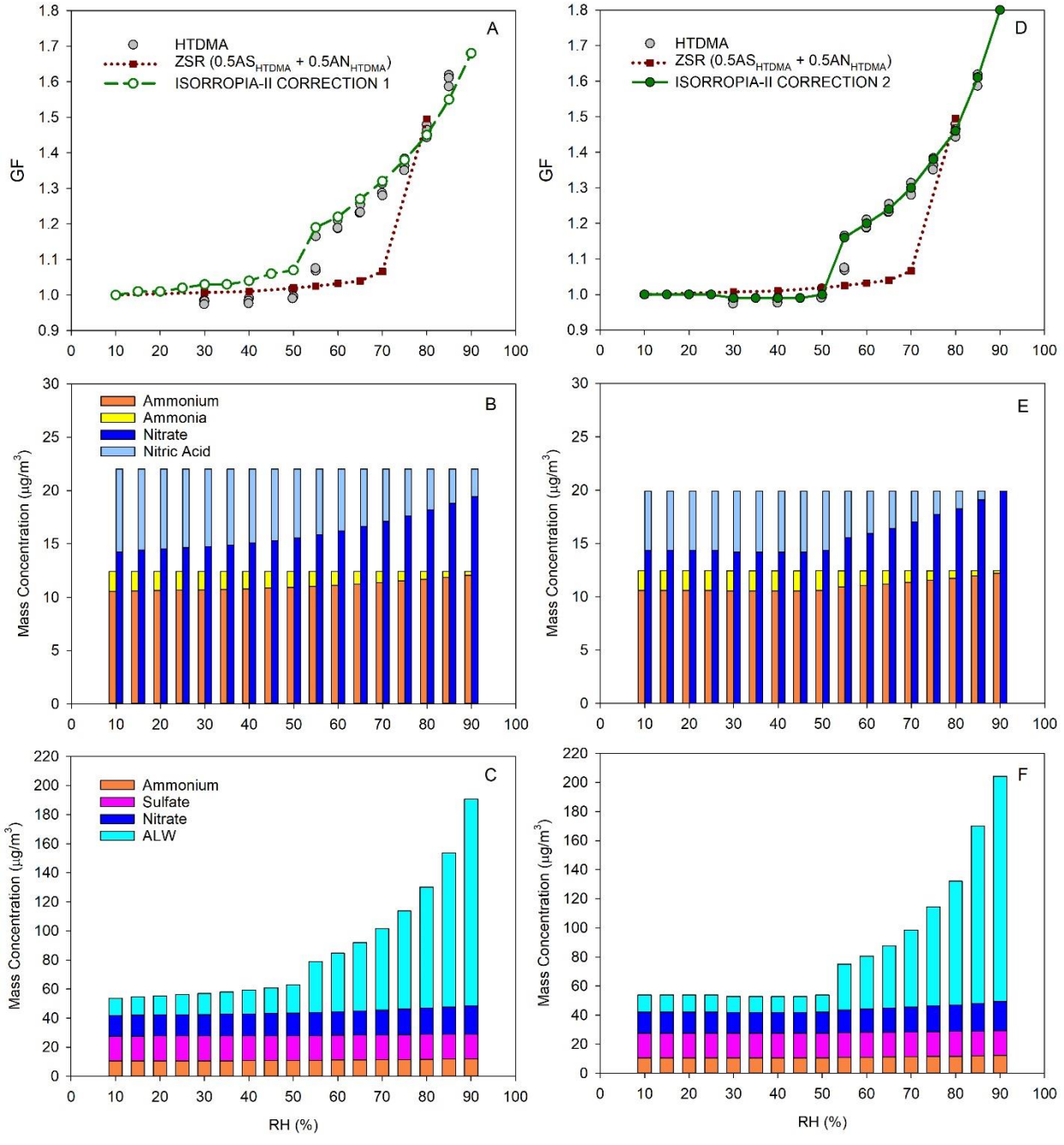

Figure 5: GF vs. RH plots for the mixture aerosols with the mass-based ratios of ammonium sulfates and ammonium nitrates to be 50 : 50 (A, and D). The gas-particle partitioning of ammonium$_{(p)}$-ammonia$_{(g)}$ and nitrate$_{(p)}$-nitric acid$_{(g)}$ (B and E). The mass concentrations of ammoniums, sulfates, nitrates and ALW in the mixture aerosols vs. RH (C and F).

https://doi.org/10.5194/acp-2022-364
Preprint. Discussion started: 30 May 2022

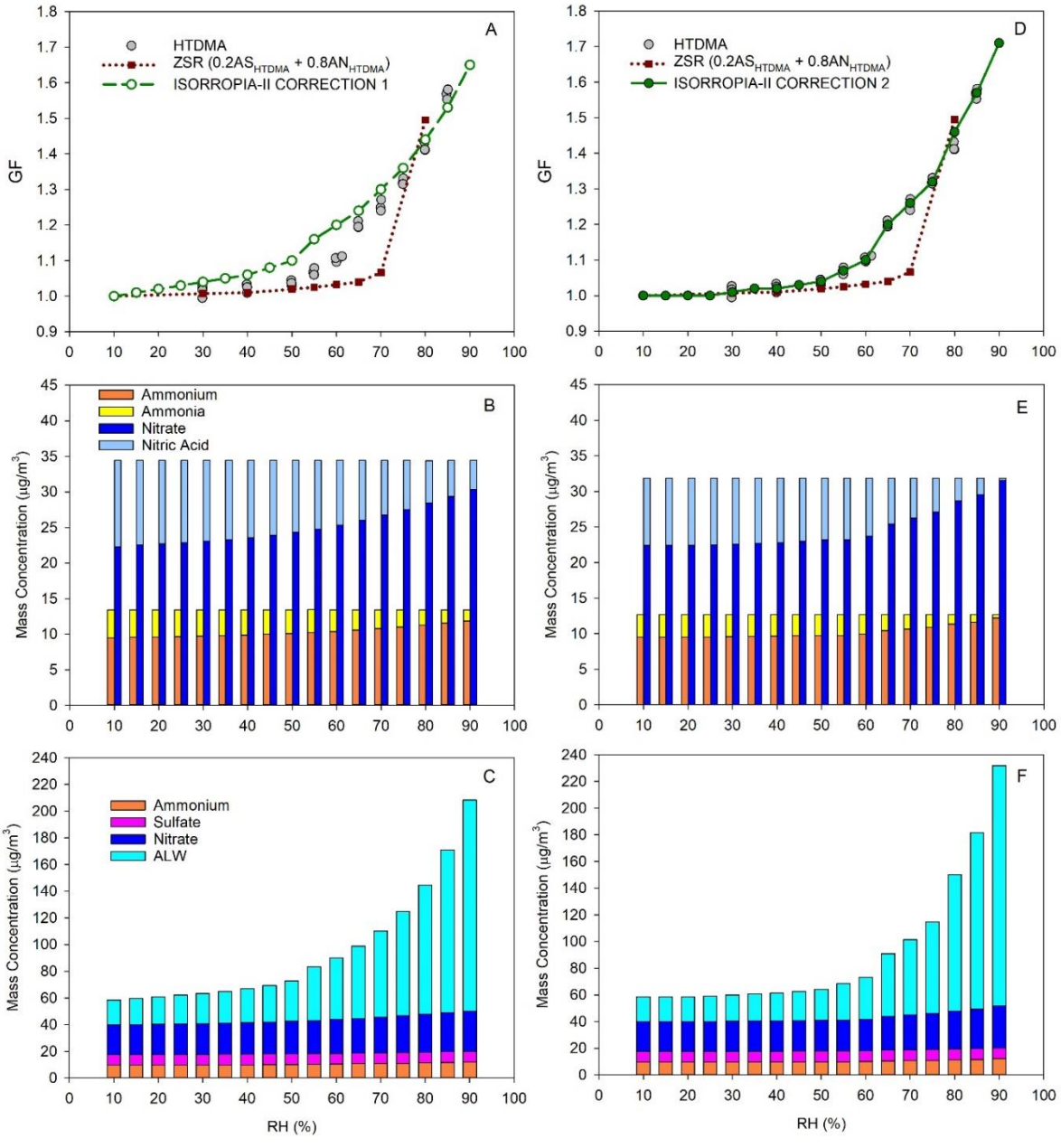

Figure 6: GF vs. RH plots for the mixture aerosols with the mass-based ratios of ammonium sulfates and ammonium nitrates to be 20 : 80 (A, and D). The gas-particle partitioning of ammonium$_{(p)}$-ammonia$_{(g)}$ and nitrate$_{(p)}$-nitric acid$_{(g)}$ (B and E). The mass concentrations of ammoniums, sulfates, nitrates and ALW in the mixture aerosols vs. RH (C and F).

https://doi.org/10.5194/acp-2022-364
Preprint. Discussion started: 30 May 2022

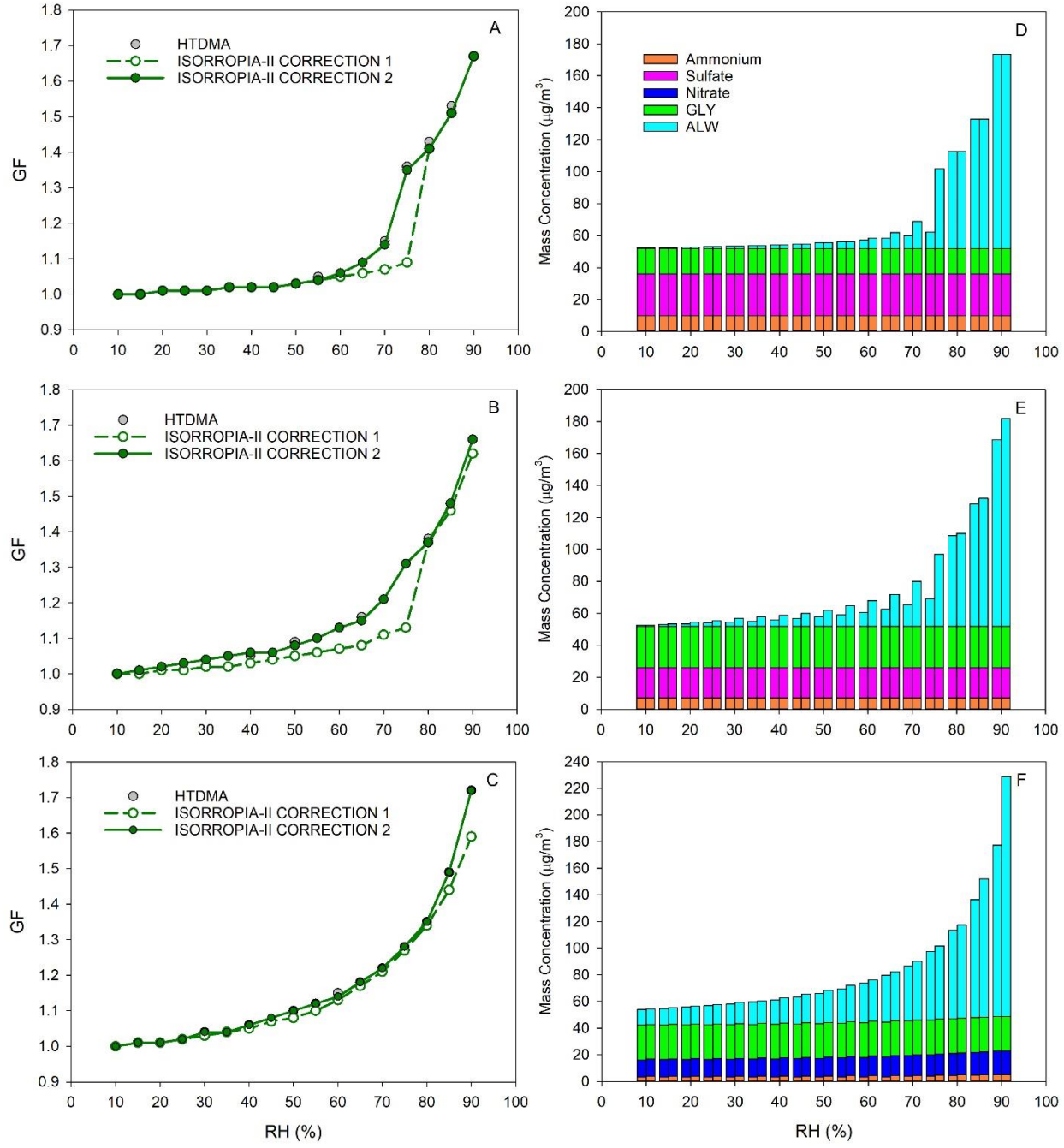

Figure 7: GF vs. RH plots for the mixture of AS and glyoxal aerosols (70 : 30) (A), the mixture of AS and glyoxal aerosols (50 : 50) (B) and the mixture of AN and glyoxal aerosols (50 : 50) (C). HTDMA indicates HTDMA measurements. Mass concentrations of aerosol components vs. RH plots (D) for (A), (E) for (B), and (F) for (C). The left stacked bar indicates ISORROPIA-II CORRECTION 1 (green open circle), and the right stacked bar indicates ISORROPIA-II CORRECTION 2 (green solid dot).

https://doi.org/10.5194/acp-2022-364
Preprint. Discussion started: 30 May 2022

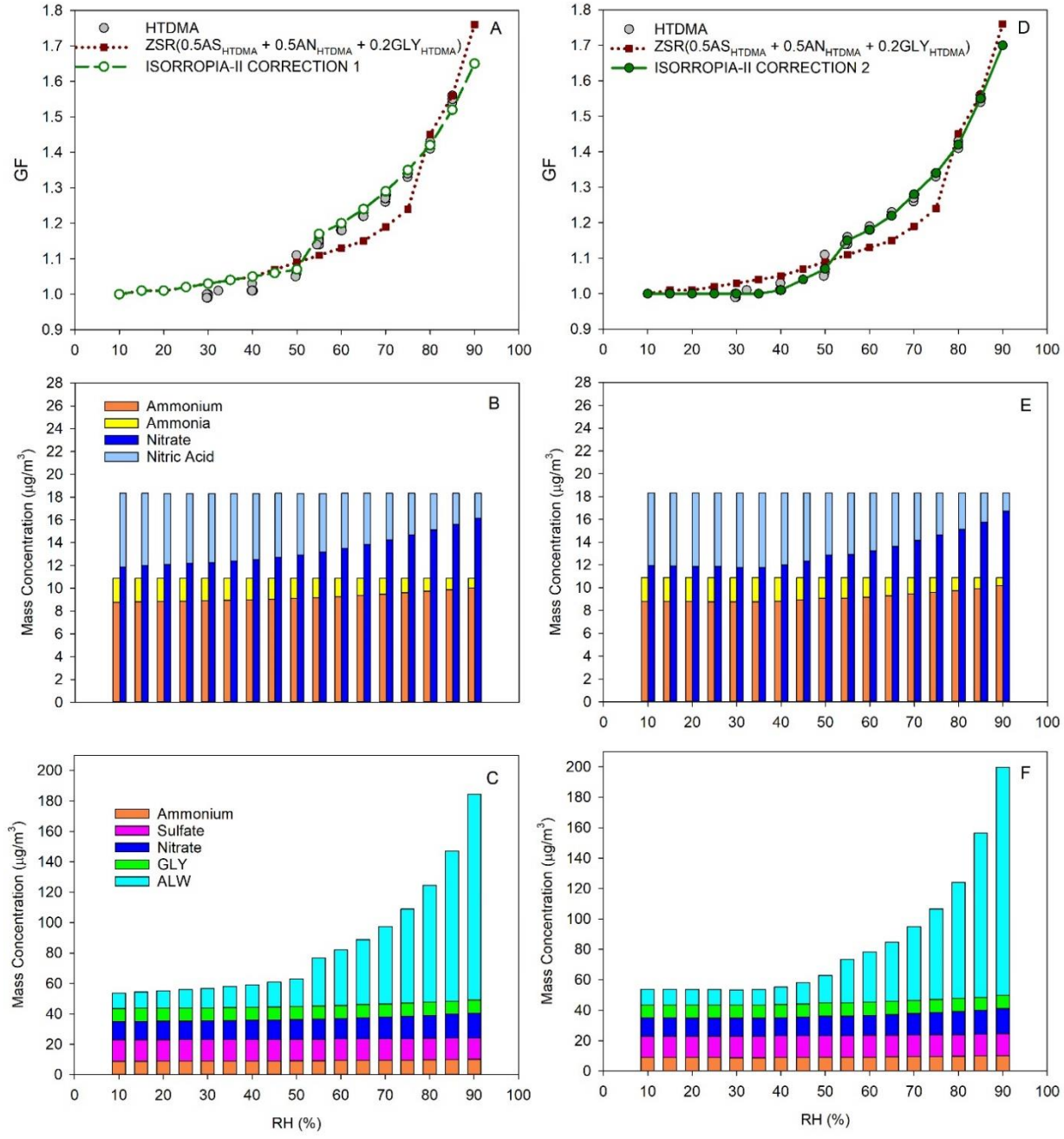

Figure 8: GF vs. RH plots for the mixture of AS, AN and glyoxal aerosols (50 : 50 : 20) (A and D). HTDMA indicates HTDMA measurements. ZSR(mAS$_{HTDMA}$ + nAN$_{HTDMA}$ +l GLY$_{HTDMA}$) indicates that the sum of HTDMA measurements for AS, AN, and glyoxal with ZSR method and the ratio (AS : AN : GLY = m : n : l). Mass concentrations of aerosol components vs. RH plots (B and C) for (A) and (E and F) for (D).